

FLEXURAL BEHAVIOR OF REINFORCED LIGHTWEIGHT AGGREGATE CONCRETE BEAMS

H S Lim¹, T H Wee¹, M A Mansur² and K H Kong¹

¹Department of Civil Engineering
Faculty of Engineering, National University of Singapore
10 Kent Ridge Crescent, Singapore 119260.
E-mail: engp0533@nus.edu.sg

²Faculty of Civil Engineering, Universiti Teknologi Malaysia, Skudai, 81310 Johor, Malaysia

ABSTRACT: The research work reported in this paper deals with the flexural response of reinforced lightweight aggregate concrete (LWAC) beams. It consists of testing a total of 11 prototype beams designed to cover a wide range of parameters and address the major design issues, like cracking and crack width, stiffness and deflection and, strength and ductility. The results of these tests, presented and discussed in relation to the use of conventional normal weight concrete (NWC) and a major structural code ACI 318, indicate that the overall response of the LWAC beams used in this study with a density of 1850 kg/m³ closely resembles that of NWC beams and that the major structural code that contain provisions for the use of LWAC give reasonable predictions. The findings of this study should therefore serve as an encouragement for the regional building authorities to consider the use of LWAC to reap its potential benefits.

Keywords: beams (reinforced concrete); flexure; lightweight concrete; serviceability; strength.

1. INTRODUCTION

The commercial demand for light, yet strong, concrete has increased many folds in recent years because of its inherent economies and advantages over conventional concrete in a variety of structural applications. Numerous lightweight concrete (LWC) structures, ranging from low-rise bungalows to multistory buildings, bridges and flyovers to marine and offshore structures can now be found in many parts of the world. ACI Committee 514 has given a comprehensive summary of major structural applications of LWC and its future application potentials. Unfortunately, the South East Asian region where we belong is yet to experience large-scale structural applications of LWC. There are two main reasons for LWC not being so popular here. First, there is a general lack of understanding on the production technique of this material, which requires greater skills and technology back up than ordinary normal weight concrete (NWC). Secondly, the information available locally on the structural performance of this material is insufficient to provide adequate guidance and confidence to the designers.

In an attempt to overcome these hurdles, a comprehensive research program has been undertaken at the National University of Singapore. The contents of this paper constitute a part of the global investigation. It deals with the overall flexural response of reinforced lightweight aggregate concrete (LWAC) beams under flexural loading.

In flexure, all the major codes of practices (ACI 318, BS 8110 and EC2) now contain rules for the design of LWC members. But a thorough search of existing literature reveals that these rules are mainly based either on research work conducted in the 1960s, subsequent to which material technology has advanced significantly, or on works that remained mostly unpublished or inaccessible to others. Although there are several reported works in recent

years (Swamy and Lambert, 1984; Ahmad and Barker, 1991; and Ahmad and Batts, 1991), the coverage given was very limited. Therefore, there is a need to critically reassess the existing code provisions in the perspective of the advances in material technology during the last two decades in a backdrop of local conditions to build designer's confidence. The research work reported in this paper has been basically directed towards achieving this goal.

2. TEST PROGRAM

The present experimental program consists of 11 prototype beams. The program and the details of test beams are presented in Table 1 and Fig. 1.

Table 1. Details of test beams and parameters studied

| Beam No. | Type of concrete | f'_c (MPa) | Tension bars* | Compn . bars* | Link (flexural zone) | $(\rho - \rho') / \rho_{bal}$ | Parameter | | | | |
|----------|------------------|--------------|---------------|---------------|----------------------|-------------------------------|-----------|--------|----------|----------|---|
| | | | | | | | CT | f'_c | A_{st} | A_{sc} | s |
| 1 | NWC | 36 | 2-T16 | 2-T10 | T10 at 130 | 0.28 | I | | | | |
| 5 | LWAC | 36 | 2-T13 | 2-T10 | T10 at 130 | 0.12 | | | III | | |
| 7 | | 35 | 2-T20 | 2-T10 | T10 at 130 | 0.55 | | | III | | |
| 8 | | 36 | 2-T16 | 2-T10 | T10 at 130 | 0.28 | I | II | III | | |
| 14 | | 41 | 4-T16 | 2-T10 | T10 at 130 | 0.74 | | | | IV | v |
| 15 | | 43 | 4-T16 | 2-T10 | T10 at 90 | 0.72 | | | | | v |
| 16 | | 43 | 4-T16 | 2-T10 | T10 at 50 | 0.72 | | | | | v |
| 17 | | 42 | 4-T16 | 2-T13 | T10 at 130 | 0.61 | | | | IV | |
| 18 | | 42 | 4-T16 | 2-T16 | T10 at 130 | 0.45 | | | | IV | |
| 19 | | 59 | 2-T16 | 2-T10 | T10 at 130 | 0.21 | | II | | | |
| 26 | | 74 | 2-T16 | 2-T10 | T10 at 130 | 0.16 | | II | | | |

NOTE: CT: type of concrete; f'_c : concrete strength; A_{st} : amount of tensile steel; A_{sc} : amount of compression steel; s : links in the flexural zone; ρ = tensile steel ratio; ρ' = compressive steel ratio; ρ_{bal} = balanced steel ratio.
* Yield strengths of T20, T16, T13 and T10 bars are 562, 560, 564 and 560 MPa, respectively

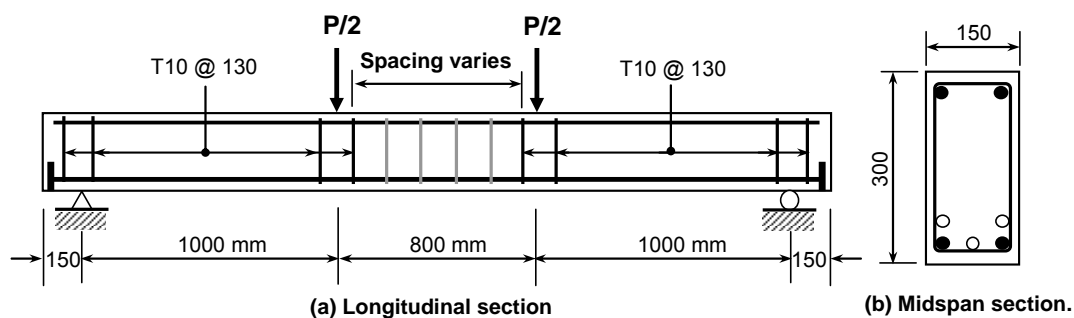


Fig. 1. Reinforcement details of test beams.

2.1 Test Specimens and Materials

All beams are rectangular in cross section, 150 mm wide and 300 mm in overall depth. They are 3100 mm long, simply supported over a span of 2800 mm and tested under two concentrated loads placed symmetrically at 800 mm apart.

The reinforcement details of the beams are shown in Fig. 1. All beams are provided with longitudinal reinforcement both in tension and compression and, with the exception of B17 and B18, may be treated as singly reinforced, but with nominal hanger bars (2-T10), to be more representative of the practical situation. Beams B17 and B18 are doubly reinforced. The longitudinal tension bars are anchored at each end by welding a bearing plate to ensure adequate anchorage. As can be seen in Table 1, the number and sizes of bars are varied among the beams to give adequate coverage on the effects of the amount of tension and compression reinforcement. The number of compression bars was two for all beams, whereas those in tension consisted of either two or four. Whenever the tension side contains four bars, they were arranged in two layers with clear gap of 25 mm in between.

Transverse reinforcement consists of T10 bars, bent into closed stirrups with spot welding at the free ends, and the same size of stirrups was used with a clear concrete cover of 20 mm on all sides throughout the test program. All beams were provided with the same spacing of stirrups in the shear zone sufficient enough to ensure flexural failure prior to any shearing distress. In the flexural zone, the amount of transverse reinforcement was varied by varying the spacing of stirrups. Most of the flexural zone were provided with a spacing of 130 mm, assumed to be nominal to avoid premature failure of the beams due to buckling of the compression bars. Closer spacing of 90 mm and 50 mm were used for the stirrups in Beams B15 and B16, respectively to investigate the effect of confinement of the concrete in the compression zone on ductility of the beam. The beams may be divided into five groups for investigating each study parameter and are labeled as I, II, III, IV & V in Table 1. The parameters being studied for the general beam behaviors are the effect of the type of concrete (NWC vs. LWAC), LWAC compressive strength, tensile & compressive steel reinforcement ratios and volumetric ratios of lateral tie reinforcement. The cube compressive strength of LWAC used consists of 40 MPa, 60 MPa and 80 MPa. The tensile steel reinforcement ratios being studied are $\rho-\rho'/\rho_{bal}$ of 0.12 (2T13), 0.28 (2T16) and 0.55 (2T20) with ρ , ρ' and ρ_{bal} being the ratio of tensile, compressive and balanced steel reinforcement contents respectively. The effect of presence of compressive steel reinforcement in the flexural zone of the beams is investigated by comparing ρ'/ρ_{bal} of 0.18 (2T10), 0.3 (2T13) and 0.45 (2T16). The volumetric ratios of lateral ties in the flexural zone being studied are 1.6 % (T10 @130 mm c/c), 2.3 % (T10 @ 90 mm c/c) and 4.2 % (T10 @ 50 mm c/c).

The NWC and LWAC used in the present program were designed and prepared in-house. Lightweight expanded clay aggregate with bulk density of 800 kg/m³ (LECA 800TM) was used for LWAC. Reinforcing steel bars used were of identical type having the properties shown in Table 1. The beams were cast in plywood molds along with sufficient number of 100×200 mm cylinders for each concrete mix to determine the properties of concretes used. The cylinder compressive strengths of concrete at the time of beam test are presented in Table 1.

2.2 Instrumentation and Test Procedure

The test beams were simply supported and were subjected to two, symmetrically placed, point loads. The distance between the two loading points was kept at 800 mm and each shear span was 1000 mm. Details of the test set-up are shown in Fig. 2. The beams were suitably instrumented for measuring deflections at several locations including the midspan, curvature of the beam over a central gauge length of 450 mm, concrete and steel strains at critical locations and surface crack widths at the centerline of bottommost layer of longitudinal tensile steel.

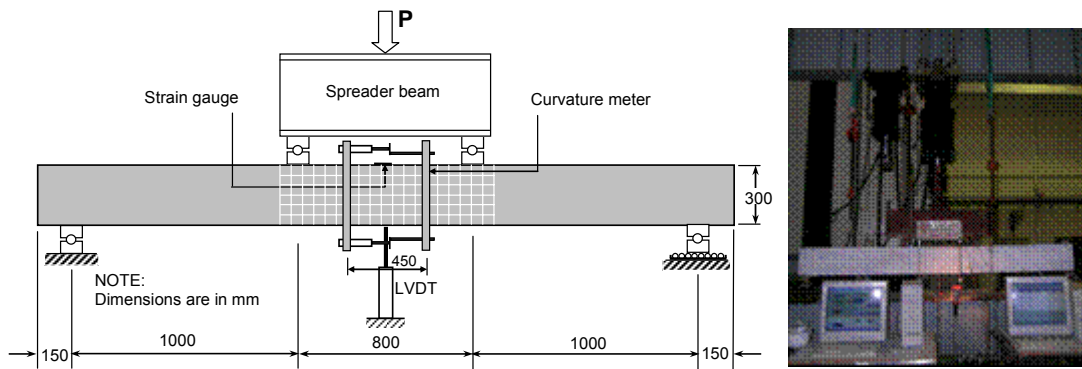


Fig 2. Test setup.

Initially, the beams were exercised by applying a load of about 5 kN and then releasing the load to overcome any slack between the specimen and the loading and support systems. All the instruments were then initialized. The beam was loaded monotonically at a rate of 0.30 mm/min up to ultimate level and then at 0.60 mm/min until failure. The load was applied by a 2000-kN servo-controlled hydraulic actuator and all deformation readings were captured by a computer at preset load intervals until final collapse.

3. TEST RESULT AND DISCUSSION

3.1 General Behavior

A typical load-deflection curve is shown in Fig. 3. It may be seen that the curve is characterized by four distinctly different segments separated by four significant events that took place during the loading process to failure. These events, labeled as A, B, C and D in Fig.3, have been identified as first cracking of the concrete, yielding of tensile reinforcement, crushing with associated spalling of the concrete cover in the compression zone and final disintegration of the compressed concrete, respectively. The first two events were associated with a reduction in the gradient of the curve, while the remaining two events led to a reduction in the applied load. In between two events, a straight line may approximate the curve. As usual, final failure occurred due to crushing and disintegration of compressed concrete, as can be seen in Fig. 4.

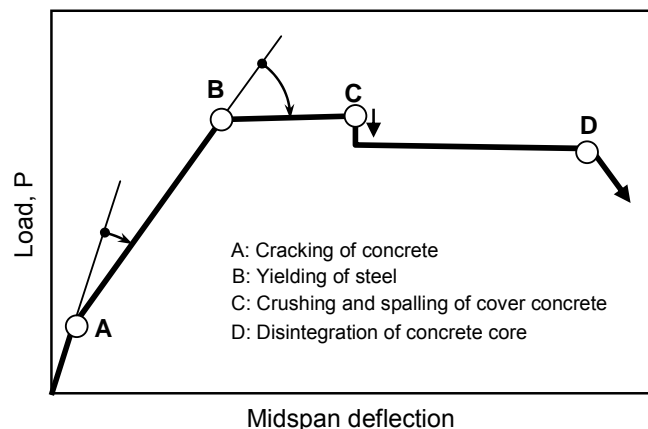


Fig. 3. Typical load-deflection curve.

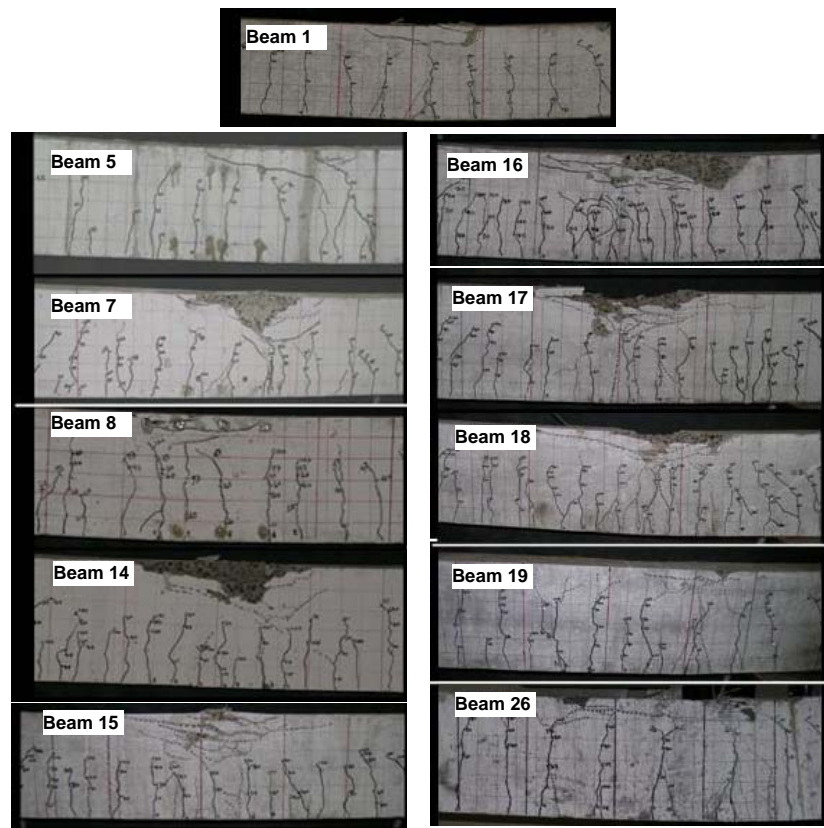


Fig. 4. Beams after failure.

All beams tested in this program behaved in a manner similar to the above description. However, as can be noted from Fig. 5, the occurrence of different events and the extent of each branch of the curve depend on the relative magnitude of the parameters investigated. It can also be noted from Figs. 5 and 6 that, for a given beam, the shape of the load-deflection curve is almost identical to that of the corresponding moment-curvature relationship and that the replacement of NWC by LWAC of same grade leads to a nearly identical response with respect to both deflection (see Fig. 5a) and midspan curvature (see Fig. 6a).

In the following discussion, experimental observations of the effects of various parameters considered in this study on cracking, service load deflection, ultimate strength and ductility are briefly highlighted for LWAC beams.

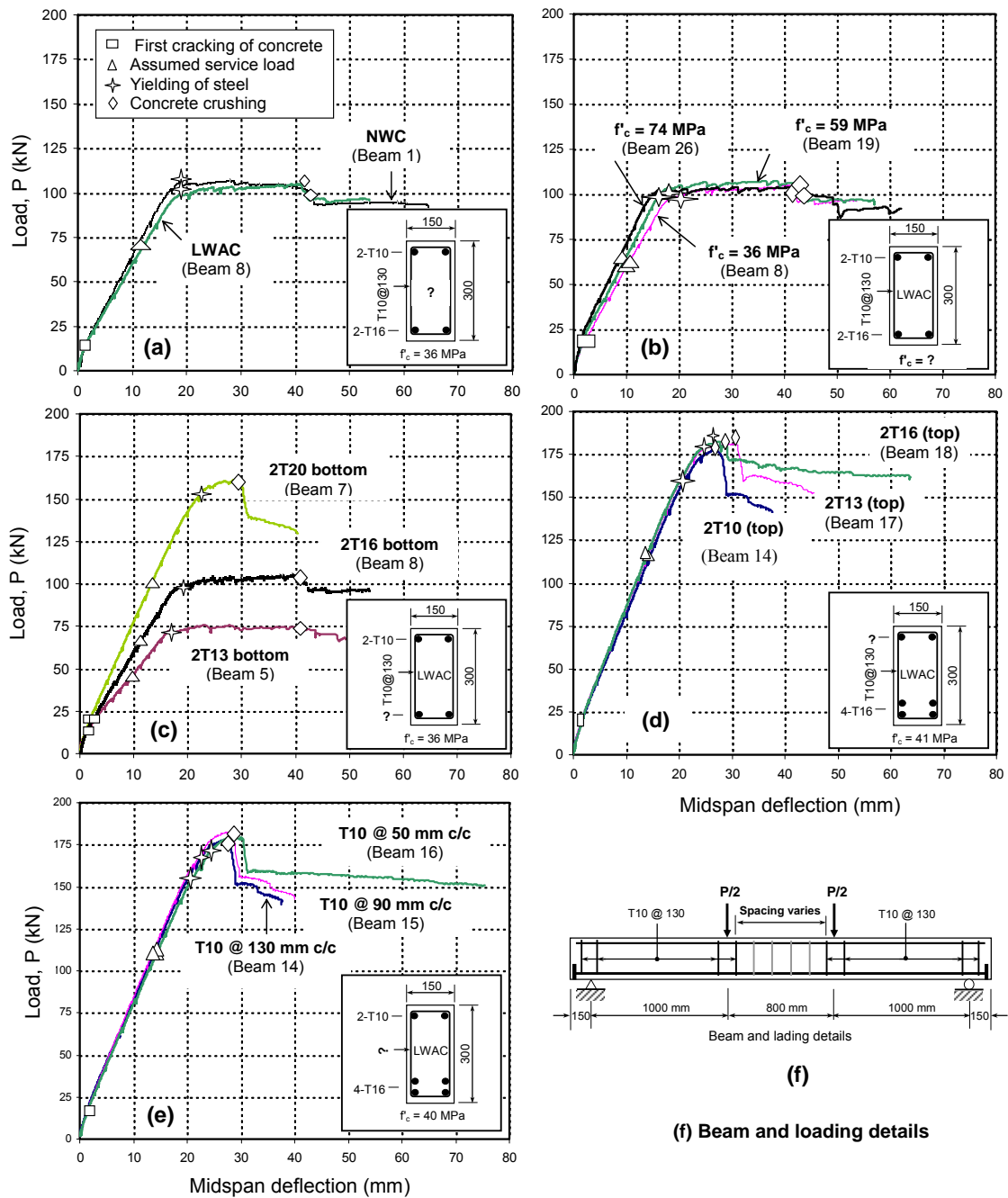


Fig. 5. Load-deflection curves of test beams. Effects of (a) concrete type (b) concrete strength (c) tensile steel ratio (d) compressive steel ratio, and (e) spacing of links in the flexural zone..

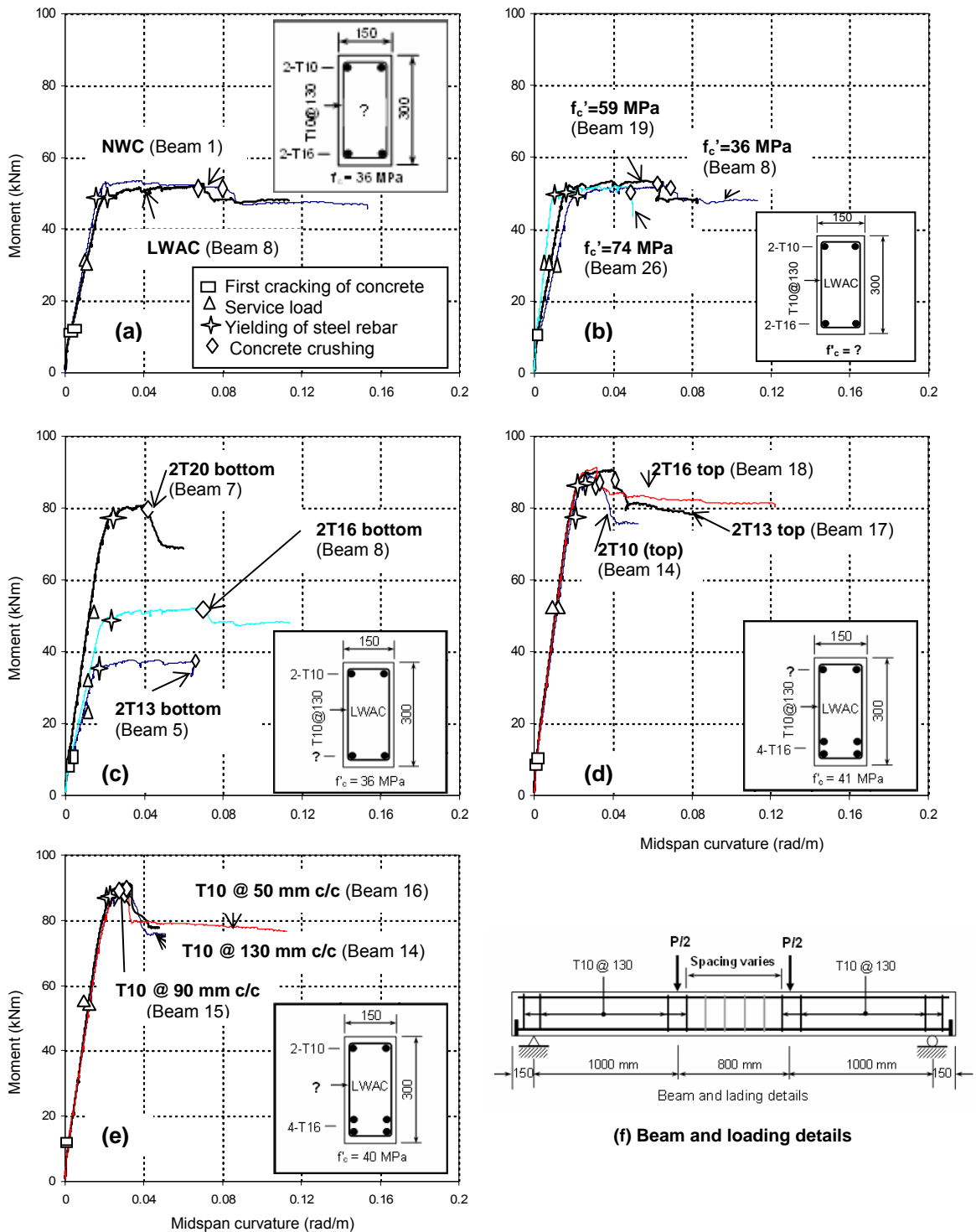


Fig 6. Moment-curvature relationships of test beams. Effects of (a) concrete type (b) concrete strength (c) tensile steel ratio (d) compressive steel ratio, and (e) spacing of links in the flexural zone.

3.2 Cracking and maximum crack width

Flexural cracking within the central region of the beam represents the first significant event that results in a change in the direction of the load-deflection curve. The loads at first cracking of the beams are shown in Table 2. A careful assessment of these values reveals that the formation of flexural cracking is primarily affected by concrete strength and the amount of tensile reinforcement; an increase in either delays the formation of cracking.

Table 2. Test results at first cracking and at assumed service load

| Beam No. | At first cracking | | At assumed service load* | | |
|----------|---------------------|-------------------------------------|--------------------------|---------------------------------|----------------------------------|
| | Load, P_{cr} (kN) | Max. Deflection, δ_{cr} (mm) | Load, P_s (kN) | Max. deflection δ_s (mm) | Max. crack width, w_{max} (mm) |
| 1 | 17.2 | 1.4 | 66.7 | 10.3 | 0.23 |
| 5 | 12.1 | 1.1 | 47.2 | 10.1 | - |
| 7 | 21.1 | 2.1 | 101.0 | 13.4 | - |
| 8 | 21.9 | 2.8 | 65.7 | 11.2 | 0.18 |
| 14 | 17.1 | 1.4 | 111.2 | 13.9 | 0.15 |
| 15 | 18.1 | 1.6 | 114.2 | 14.1 | 0.20 |
| 16 | 17.1 | 1.6 | 112.3 | 14.7 | 0.18 |
| 17 | 17.1 | 1.3 | 113.3 | 13.8 | 0.25 |
| 18 | 17.2 | 1.5 | 114.0 | 13.6 | 0.20 |
| 19 | 18.3 | 1.8 | 67.4 | 10.4 | 0.25 |
| 26 | 20.1 | 1.5 | 64.9 | 8.8 | 0.30 |

* Assumed service load, $P_s = \text{Test ultimate load, } P_u / 1.6$

Fig. 4 shows the cracking patterns within the test zone of central 800 mm of the beams. It may be seen that all beams exhibited similar cracking patterns. However, a closer look reveals that the beams containing 4T16 bars (highest amount of reinforcement used in this study) displayed more number of cracks or, in other words, closer crack spacing when fully developed.

The effects of the type of concrete, concrete strength, tensile reinforcement ratio and compressive reinforcement ratio on the development of maximum crack width at the level of tension reinforcement are presented in Figs, 7(a), (b), (c), and (d), respectively. It can be seen that the parameter that provides distinct and conclusive evidence of slower growth of cracks is the amount of tension reinforcement; higher amount being more effective at a given load level.

The design criterion with regard to cracking is the maximum crack width at service load. In this study, service load is assumed as the test ultimate load divided by a factor of 1.6. The maximum crack widths at effective depth of the beams at service load levels are shown in Table 2. It can be observed that at this load, the average maximum crack width is about 0.22 mm, the largest and smallest being 0.3 mm and 0.15 mm, respectively. Beam 26, that contained 2T16 bars in tension combined with a concrete of compressive strength, $f'_c = 74$ MPa demonstrated the largest, while Beam 14 with 4T16 tension bars and $f'_c = 41$ MPa displayed the smallest maximum crack width at the assumed service load. The effects of other parameters could hardly be distinguished.

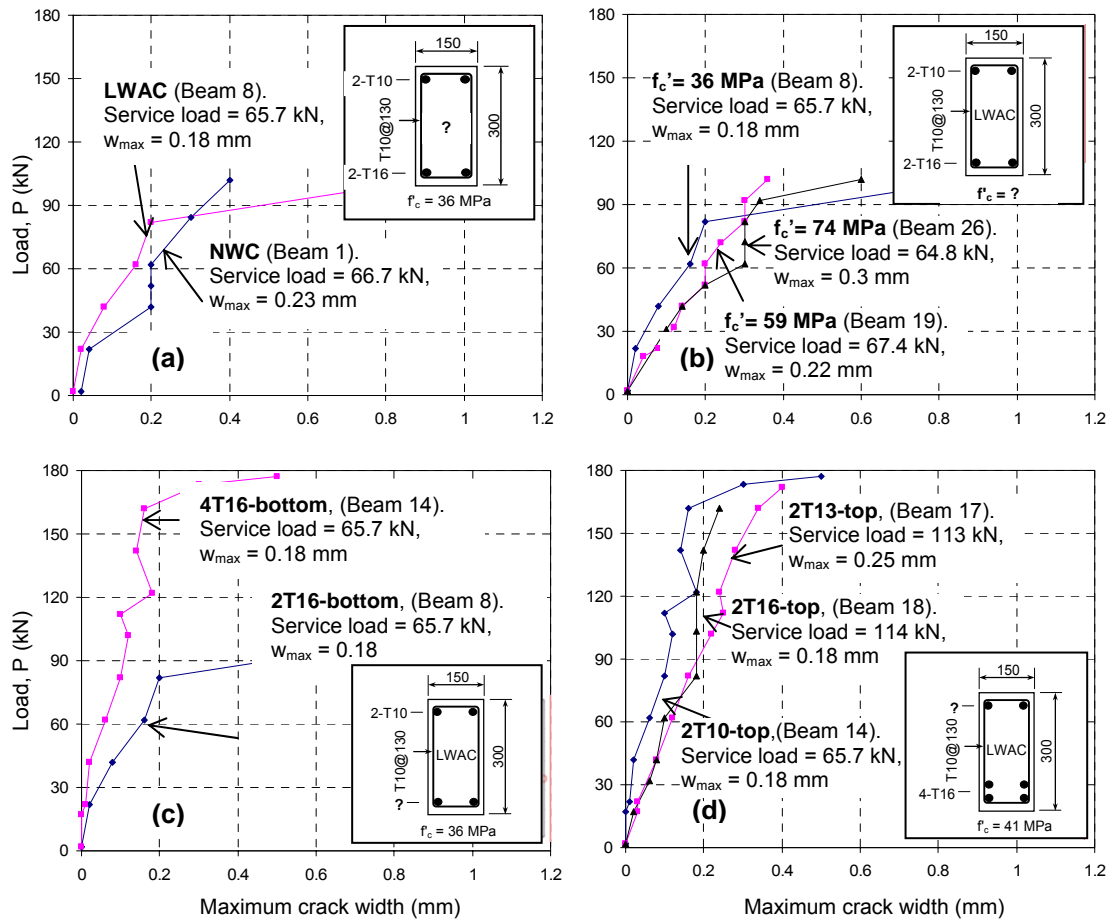


Fig 7. Development of maximum crack width at effective depth of test beams. Effects of (a) concrete type (b) concrete strength (c) tensile steel ratio (d) compressive steel ratio.

3.3 Stiffness and Service Load Deflection

The gradient of the load-deflection or moment-curvature relationship is an indication of beam stiffness. It may be seen in Fig. 5 and Fig. 6 that prior to cracking, the stiffness of the beams remained practically the same for the entire set of parameters and their ranges considered in this study. However, there was some variation in the gradient of the curve between cracking (Event A) and yielding of steel (Event B). LWAC beam, Beam 8, demonstrated slightly smaller post-cracking stiffness than the corresponding NWC beam (Fig. 5a). The post-cracking stiffness has been found to increase either with an increase in concrete strength (Fig. 5b) or with an increase in the amount of tension reinforcement (Fig. 5c); the effect of the later being more pronounced. The effect of the amount of compression reinforcement or the spacing of stirrups in the flexural zone has practically no influence on beam stiffness.

The maximum (midspan) deflection, δ_s , obtained experimentally at the assumed service load, P_s are presented in Table 2. It ranges from about 9 mm to about 15 mm, the smallest deflection being displayed by the high strength concrete beam, Beam 26.

3.4 Ultimate Strength and Failure Modes

The ultimate (maximum) strengths attained by the beams may be read either from the load-deflection curves of Fig. 5 or moment-curvature relationships of Fig. 6, the numerical values

being presented in Table 3. It may be seen that, among the various parameters considered in this study, only the amount of tension reinforcement has the most noticeable influence on ultimate strength for obvious reasons.

In all beams attainment of ultimate strength was accompanied by crushing of the concrete (Event C) and a sudden drop in the applied load. The maximum compressive strain in concrete recorded at ultimate load ranges from 0.0026 to 0.0038 (see Table 3) with no definite trend. All beams failed in the usual flexural mode by yielding of steel and crushing of the concrete in the compression zone as can be seen in Fig. 4.

Table 3. Test results at yielding of steel reinforcement and at ultimate load

| Beam No. | Ultimate load, P_u (kN) | Midspan deflection | | Midspan curvature | | Max. concrete comp. strain, ϵ_{cu} | Curvature ductility, $\Psi_d = (\phi_u/\phi_y)$ | Deflection ductility, $\mu_d = (\delta_u/\delta_y)$ |
|----------|---------------------------|------------------------------|---------------------------------------|-------------------------------|----------------------------------------|---------------------------------------------|-------------------------------------------------|-----------------------------------------------------|
| | | At ultimate, δ_u (mm) | At yielding of steel, δ_y (mm) | At ultimate, ϕ_u (rad/m) | At yielding of steel, ϕ_y (rad/m) | | | |
| 1 | 103.0 | 40.5 | 18.2 | 0.0769 | 0.0158 | 0.00374 | 4.86 | 2.23 |
| 5 | 73.2 | 41.1 | 16.3 | 0.0655 | 0.0154 | 0.00318 | 4.26 | 2.52 |
| 7 | 161.5 | 29.8 | 22.8 | 0.0401 | 0.0220 | 0.00317 | 1.82 | 1.31 |
| 8 | 104.9 | 41.0 | 18.4 | 0.0704 | 0.0202 | 0.00382 | 3.48 | 2.22 |
| 14 | 173.8 | 27.9 | 21.1 | 0.0333 | 0.0203 | 0.00318 | 1.64 | 1.32 |
| 15 | 182.1 | 28.7 | 22.7 | 0.0332 | 0.0213 | 0.00287 | 1.56 | 1.26 |
| 16 | 177.3 | 30.5 | 24.8 | 0.0326 | 0.0237 | 0.00339 | 1.37 | 1.23 |
| 17 | 180.3 | 31.1 | 23.5 | 0.0404 | 0.0225 | 0.00351 | 1.80 | 1.32 |
| 18 | 181.3 | 27.8 | 26.0 | 0.0319 | 0.0275 | 0.00259 | 1.16 | 1.07 |
| 19 | 104.7 | 43.1 | 17.1 | 0.0652 | 0.0163 | 0.00325 | 4.00 | 2.52 |
| 26 | 103.1 | 41.5 | 16.2 | 0.0500 | 0.0111 | 0.00269 | 4.50 | 2.57 |

3.5 Deformation and Ductility

As discussed earlier, the load-deformation curves obtained experimentally may be generalized in the form shown in Fig. 3. It may be seen that the curves between yielding of steel (Event 2) and crushing and spalling of concrete cover in compression is nearly horizontal indicating the ability of the beam to deform without losing strength. This is an indication of ductility, defined as the ability of a member to deform at approximately the same load. It may be measured at various levels of a structure - material, section, element or global. In this study, only sectional ductility and element ductility are of concern. ratio of curvature or deflection at crushing of the concrete to that at yielding of steel gives the numerical value of ductility, known as ductility index. The curvature ductility index, Ψ_d , and deflection ductility index, μ_d , for the beams tested in this program are presented in Table 3. It may be seen that For the LWAC beams, curvature ductility index ranges from 1.16 to 4.50, while that for deflection varies from 1.07 to 2.57.

A close review of Figs. 5 and 6 clearly shows the effect of various parameters on ductility. It may be seen that, keeping other parameters constant, replacement of normal-weight aggregates by light-weight aggregates has no noticeable influence on ductility. Similar to NWC beams, an increase in concrete strength leads to higher ductility (Fig. 8a), but for the range of parameters used in this study, this increase is only marginal. The most significant effect on ductility is afforded by tensile reinforcement. A decrease in the amount of tensile reinforcement dramatically improves ductility (Fig. 8b). Use of higher amount of compression reinforcement or closer stirrups in the flexural zone improves the post-crushing response of

the beam in terms of lesser drop in the applied load at crushing of the concrete and the extent of subsequent deformation without significant loss of strength (See Figs. 5 and 6)..

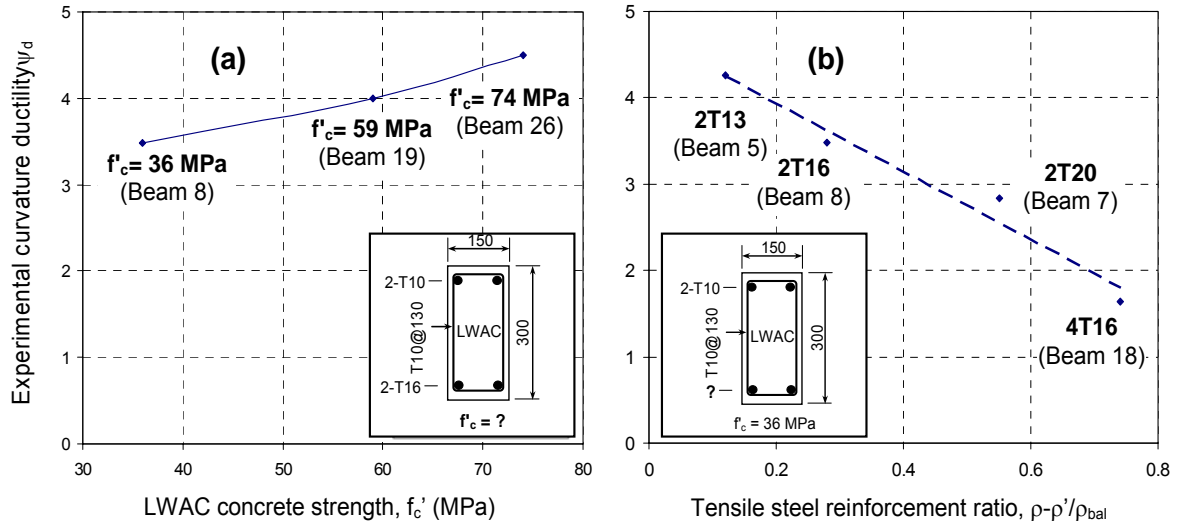


Fig 8. Effects of (a) concrete strength, f'_c and (b) tensile steel ratio on curvature ductility of LWAC beams.

3.6 Comparison with Code Provisions

The load-deformation response of all the 11 beams at critical events, such as cracking, yielding of steel, and crushing of concrete (ultimate) are calculated analytically using the conventional flexural theory supported by the ACI 318-05 Code (2005), in which three fundamental principles of mechanics – equilibrium, compatibility and material laws are satisfied. In the analysis, however, concrete is assumed to be elastic up to yielding of steel, and is represented by the rectangular stress block at ultimate. Material parameters like modulus of rupture, f_r , elastic modulus, E , stress block shape factors, ultimate concrete compressive strain, ϵ_{cu} (failure criterion) etc. are taken from ACI 213 and ACI 318 code provisions for NWC or LWAC, wherever appropriate. For steel, a bi-linear stress-strain relationship is used using the strength and elastic modulus determined experimentally. However, most of the research addressing performance of structural lightweight concrete that form the basis for existing ACI 318 code requirements are limited to concrete with compressive strength less than 41 MPa. Therefore, whenever concrete strength exceeds 41 MPa, the material parameters determined as part of the overall program are used to comply with the ACI 213R-03 code, which states that the parameters used should be based on tests conducted on the selected materials..

The calculated strengths at cracking, yielding and ultimate are presented and compared with the respective experimental values in Table 4. It can be seen that the conventional code method can predict the ultimate and yielding strength quite accurately. However, the experimental cracking strength is on the average 12 % more than the theoretical values.

Table 4. Comparison of experimental loads at cracking, yielding of steel and at ultimate with the predictions of the ACI 318-05 code

| Beam No. | Calculated load, P (kN) from flexural theory and ACI 318-05 code | | | Ratio experimental load / load from code | | |
|--------------------|------------------------------------------------------------------|------------------|----------------------|------------------------------------------------------|----------------------------------------------------|----------------------------------------------------|
| | 1st. crack, P_{cr}^{**} | 1st yield, P_y | Ultimate load, P_u | $\frac{P_{cr, \text{expt}}}{P_{cr, \text{ACI 318}}}$ | $\frac{P_{y, \text{expt}}}{P_{y, \text{ACI 318}}}$ | $\frac{P_{u, \text{expt}}}{P_{u, \text{ACI 318}}}$ |
| 1 | 19.0 | 105.1 | 108.0 | 0.91 | 1.00 | 0.95 |
| 5 | 13.7 | 69.4 | 71.6 | 0.88 | 1.03 | 1.02 |
| 7 | 15.5 | 158.7 | 161.9 | 1.36 | 0.97 | 1.00 |
| 8 | 14.4 | 104.0 | 108.0 | 1.52 | 0.94 | 0.97 |
| 14 | 16.4 | 188.3 | 189.6 | 1.04 | 0.85 | 0.92 |
| 15 | 16.5 | 188.4 | 190.4 | 1.10 | 0.91 | 0.96 |
| 16 | 16.5 | 188.4 | 190.4 | 1.03 | 0.91 | 0.93 |
| 17 | 16.8 | 188.6 | 193.0 | 1.02 | 0.93 | 0.93 |
| 18 | 17.1 | 188.2 | 194.3 | 1.01 | 0.96 | 0.93 |
| 19 | 17.7 | 104.7 | 109.7 | 1.03 | 0.97 | 0.95 |
| 26 | 19.5 | 105.0 | 110.2 | 1.03 | 0.97 | 0.94 |
| Mean | | | | 1.09 | 0.95 | 0.95 |
| Standard deviation | | | | 0.19 | 0.05 | 0.03 |

** 1st cracking load is calculated from $f_r = 0.62(f_c')^{0.5}$ for NWC and $f_r = 0.44(f_c')^{0.5}$ for LWAC.
 $E = w_c^{1.5} 0.043 \sqrt{f_c'}$ is used for NWC and LWC. w_c is concrete density and valid from 1440 to 2480 kg/m³.

The theoretical midspan deflection at first cracking, assumed service load and at yielding of steel reinforcement load are presented and compared with the respective experimental deflection in Table 5.. It may be seen that the experimental deflections are on the average 37 % more than the theoretically computed values obtained by using elastic flexural theory supported by ACI 318 (that is, $\Delta = 0.1ML^2/EI_c$). Also, the experimental midspan deflection at first cracking and at yielding of steel reinforcement is 87 % and 41 % more than that predicted. Results indicate that the elastic flexural theory supported by ACI 318 code underestimates the actual deflection for both NWC and LWAC beams. However,, Ahmed and Batts (1991) have shown that the calculation of deflection based on numerical integration of curvatures at several sections along the length of the beam can accurately predict maximum deflection at service load. Therefore, the current simplified approach of computing service load deflection contained in the ACI Code needs a thorough review.

Table 6 compares the midspan curvatures obtained experimentally at various stages of loading with the corresponding values computed theoretically. It shows that the experimental midspan curvature is, on the average, about 10 % larger than the predicted values for loading stages corresponding to first cracking of concrete, assumed service load and yielding of steel, and is 20 % smaller at ultimate stage of loading..

Table 7 shows a comparison of curvature ductility obtained experimentally with the respective computed values. It may be seen that the curvature ductility of the beams can be predicted with reasonable accuracy, except for four beams. The ratio of experimental to calculated curvatures falls below 0.71 for beams 5, 18, 19 and 26. The probable reason for such a wide variation could not be identified at this stage of the study. A thorough scrutiny of experimental data, together with the bases of theoretical formulations for curvature calculations is therefore necessary.

Table 5. Comparison of midspan deflections at various loading stages with the predictions of the ACI 318-05 code

| Beam No. | Calculated midspan deflection, Δ (mm) from flexural theory and ACI 318-05 code | | | Ratio experimental midspan deflection / midspan deflection from code | | |
|--------------------|---------------------------------------------------------------------------------------|---------------------------|----------------------|----------------------------------------------------------------------|-------------------------------------------------------|-------------------------------------------------------|
| | 1st crack, Δ_{cr}^{**} | Service stage, Δ_s | Yielding, Δ_y | $\delta_{cr, \text{expt}} / \Delta_{cr, \text{ACI318}}$ | $\delta_{s, \text{expt}} / \Delta_{s, \text{ACI318}}$ | $\delta_{y, \text{expt}} / \Delta_{y, \text{ACI318}}$ |
| 1 | 0.8 | 7.5 | 12.4 | 1.82 | 1.38 | 1.47 |
| 5 | 0.8 | 7.8 | 12.1 | 1.31 | 1.29 | 1.34 |
| 7 | 0.9 | 9.5 | 14.8 | 2.25 | 1.42 | 1.54 |
| 8 | 0.9 | 8.2 | 13.2 | 3.24 | 1.36 | 1.40 |
| 14 | 1.1 | 9.9 | 16.9 | 1.26 | 1.41 | 1.25 |
| 15 | 0.9 | 10.1 | 16.8 | 1.82 | 1.39 | 1.35 |
| 16 | 0.9 | 9.9 | 16.8 | 1.79 | 1.48 | 1.48 |
| 17 | 0.9 | 9.8 | 16.5 | 1.41 | 1.40 | 1.43 |
| 18 | 0.9 | 9.7 | 16.1 | 1.60 | 1.41 | 1.61 |
| 19 | 0.8 | 7.9 | 12.6 | 2.15 | 1.32 | 1.35 |
| 26 | 0.8 | 7.2 | 12.4 | 1.91 | 1.21 | 1.30 |
| Mean | | | | 1.87 | 1.37 | 1.41 |
| Standard deviation | | | | 0.53 | 0.07 | 0.11 |

Note: The ratio of $\delta_{u, \text{expt}} / \Delta_{u, \text{ACI 318}}$ is not computed as the expression for $\Delta_{u, \text{ACI 318}}$ is based on elastic bending theory at the midspan section where $\Delta = 0.1ML^2/EI_c$ which is not accurate for the inelastic region.

Table 6. Comparison of midspan curvatures at different loading stages with the predictions of the ACI 318-05 code

| Beam no. | Calculated midspan curvature, ϕ (rad/m) from flexural theory and ACI 318-05 code | | | | Ratio experimental midspan curvature / midspan curvature from code | | | |
|--------------------|---------------------------------------------------------------------------------------|-------------------------|---------------------------------|--------------------------|--------------------------------------------------------------------|---------------------------------------------------|---------------------------------------------------|---------------------------------------------------|
| | 1 st crack, ϕ_{cr}^{**} | Service stage, ϕ_s | 1 st yield, ϕ_y | Ultimate stage, ϕ_u | $\phi_{cr, \text{expt}} / \phi_{cr, \text{ACI318}}$ | $\phi_{s, \text{expt}} / \phi_{s, \text{ACI318}}$ | $\phi_{y, \text{expt}} / \phi_{y, \text{ACI318}}$ | $\phi_{u, \text{expt}} / \phi_{u, \text{ACI318}}$ |
| 1 | 0.0009332 | 0.00917 | 0.0152 | 0.0797 | 0.92 | 1.15 | 1.04 | 0.96 |
| 5 | 0.0009939 | 0.00955 | 0.0149 | 0.1803 | 0.69 | 0.98 | 1.03 | 0.36 |
| 7 | 0.0011296 | 0.01164 | 0.0182 | 0.0413 | 1.39 | 1.04 | 1.21 | 0.97 |
| 8 | 0.0010467 | 0.01013 | 0.0162 | 0.0797 | 2.48 | 1.15 | 1.25 | 0.88 |
| 14 | 0.0011028 | 0.01216 | 0.0208 | 0.0330 | 0.91 | 1.06 | 0.98 | 1.01 |
| 15 | 0.0010986 | 0.01242 | 0.0207 | 0.0335 | 1.11 | 1.01 | 1.03 | 0.99 |
| 16 | 0.0010986 | 0.01222 | 0.0207 | 0.0335 | 1.01 | 1.06 | 1.15 | 0.97 |
| 17 | 0.0011173 | 0.01209 | 0.0203 | 0.0402 | 0.84 | 1.01 | 1.11 | 1.01 |
| 18 | 0.0011372 | 0.01190 | 0.0199 | 0.0538 | 1.02 | 1.05 | 1.38 | 0.59 |
| 19 | 0.0009997 | 0.00968 | 0.0155 | 0.1066 | 1.25 | 0.96 | 1.05 | 0.62 |
| 26 | 0.0009821 | 0.008911 | 0.0153 | 0.1250 | 0.75 | 0.64 | 0.73 | 0.40 |
| Mean | | | | | 1.12 | 1.01 | 1.09 | 0.80 |
| Standard deviation | | | | | 0.47 | 0.14 | 0.17 | 0.25 |

Table 7. Comparison of experimental ductility with that calculated from flexural theory supported by ACI 318-05 code

| Beam No. | Experimental ductility | | Calculated curvature ductility from flexural theory supported by ACI 318-05, Ψ_{ACI318}^* | Ratio experimental curvature ductility / ACI318 code curvature ductility |
|--------------------|-------------------------------|-------------------------------|------------------------------------------------------------------------------------------------|--------------------------------------------------------------------------|
| | Curvature ductility, Ψ_d | Deflection ductility, μ_d | | $\Psi_{expt} / \Psi_{ACI318}$ |
| 1 | 4.86 | 2.23 | 5.2 | 0.93 |
| 5 | 4.26 | 2.52 | 12.1 | 0.35 |
| 7 | 1.82 | 1.31 | 2.3 | 0.79 |
| 8 | 3.48 | 2.22 | 4.9 | 0.71 |
| 14 | 1.64 | 1.32 | 1.6 | 1.03 |
| 15 | 1.56 | 1.26 | 1.6 | 0.98 |
| 16 | 1.37 | 1.23 | 1.6 | 0.86 |
| 17 | 1.80 | 1.32 | 2.0 | 0.90 |
| 18 | 1.16 | 1.07 | 2.7 | 0.43 |
| 19 | 4.00 | 2.52 | 6.8 | 0.59 |
| 26 | 4.50 | 2.57 | 8.2 | 0.55 |
| Mean | | | | 0.74 |
| Standard deviation | | | | 0.23 |

4. CONCLUDING REMARKS

Detailed test results describing the complete flexural response of 11 reinforced LWAC (density = 1850 kg/m³) beams, including one with NWC, are presented in this paper. The major parameters considered in the study include the type of concrete, compressive strength of concrete, amount of tension and compression reinforcement and spacing of stirrups in the compression zone. The results of these tests are discussed with regard to cracking and maximum crack width, deflection at service load, ultimate strength and ductility, and the effects of various parameters identified. The major experimental results are compared with the predictions of the methods contained in the American Code of Practice (ACI 318-2005 and ACI 213-2003). Within the scope of the experimental and analytical investigations reported in this paper, the following conclusions may be drawn:

1. The overall flexural response of a reinforced LWAC beam used in this study closely resembles that of an equivalent beam with NWC.
2. An increase in concrete strength increases the first cracking load significantly. It also increases the post-cracking stiffness, ultimate strength and ductility, but such an increase is only marginal.
3. Similar to NWC beams, an increase in the amount of tension reinforcement reduces the maximum crack width at service load, increases the post-cracking stiffness and ultimate strength of a beam, but drastically reduces ductility.
4. The beam response up to ultimate strength remains identical as the amount of compression steel, enclosed by nominal stirrups, is increased. However, such an increase modifies the post-crushing response. It leads to a smaller drop in the load at crushing and spalling of the concrete cover and extends the plateau of approximately the same load with increasing deformation.
5. Similar to the effect of compression reinforcement, spacing of stirrups in the flexural zone affects only the post-crushing response of the beam. Closer spacing of stirrups reduces the amount of drop in the load carrying capacity of a beam at crushing and extends the linear branch of the curve of approximately the same load with increasing deformation.

6. The methods contained in the American Code of practice (ACI 318-2005 and ACI 213-2003) for LWAC can predict the cracking and ultimate strength quite accurately. However, the methods consistently underestimate the service load deflection and overestimate ductility index in most of the cases. Hence, there is need to re-examine the background to the current recommendations of the codes for the calculation of deformations in LWAC beams.

5. ACKNOWLEDGEMENTS

The authors wish to express their gratitude and sincere appreciations to the Building and Construction Authority of Singapore (BCA) for financing this research. The authors are very grateful for the assistance rendered by the NUS Civil Engineering Laboratory Manager & Technical Staff (Mr. Lim, Mr. Sit, Mr. Ishak, Mr. Choo, Mr. Koh, Ms. Annie, Mr. Kamsan, Mr. Ang, Mr. Yip, Mr. Yong, Mr. Ow & Mr. Stanley), Research Staff (Mr. Babu, Mr. Zhu, Dr. Kannan, Mr. Kum & Ms. Myat) and VIP students (Ms. Wenjia, Ms. Lim & Mr. Camdu) at various stages of this investigation..

6. REFERENCES

- ACI Committee 213, 2003, *Guide for Structural Lightweight Aggregate Concrete*, ACI 213R-03, American Concrete Institute, U.S.A, 2003.
- ACI 318-05, 2005, *Building Code Requirements for Structural Concrete*, ACI Manual of Concrete Practice, Part 3, American Concrete Institute, U.S.A.
- Ahmad, S.H. and Barker, R., 1991, *Flexural Behavior of Reinforced High-Strength Lightweight Concrete Beams*, ACI Structural Journal, 88(1), pp 69-77.
- Ahmad, S.H. and Batts, J., 1991, *Flexural Behavior of Double Reinforced High-Strength Lightweight Concrete Beams with Web Reinforcement*, ACI Structural Journal, 88(3), pp. 351-358.
- British Standard Institution, 2002, *BS8110 Structural use of concrete-Part 1 & 2* BSI, London, May 2002.
- Comite Euro-International du Beton – Federation Internationale de la Precontrainte (CEB-FIP), 1990, *CEB-FIP Model Code*. Thomas Telford, London, UK, 1993.
- EC2, ENV 1992-1-4, 1994, *Eurocode 2: Design of concrete structures, Part 1-4: General rules-lightweight aggregate concrete with closed structures*, 1994.
- FIB Task Group 8.1 Report, 2000, *Lightweight aggregate concrete*. International Federation for Structural Concrete Lausanne, Switzerland, 2000.
- Swamy, R.N. and Lambert, G.H., 1984, *Flexural behavior of reinforced concrete beams made with fly ash coarse aggregates*, The International Journal of Cement Composites and Lightweight Concrete, Vol. 6, No. 3, Construction Press, 1984, pp 189-200.